Thin-Film Composite Cyclomatrix Poly(Phenoxy)Phosphazenes Membranes for Hot Hydrogen Separation

Radmanesh, Farzaneh; Sudhölter, Ernst J.R.; Tena, Alberto; Elshof, Maria G.; Benes, Nieck E.

DOI
10.1002/admi.202202077

Publication date
2022

Document Version
Final published version

Published in
Advanced Materials Interfaces

ADVANCED MATERIALS INTERFACES
www.advmatinterfaces.de

Thin-Film Composite Cyclomatrix Poly(Phenoxy) Phosphazenes Membranes for Hot Hydrogen Separation

*Farzaneh Radmanesh, Ernst J. R. Sudhölter, Alberto Tena, Maria G. Elshof, and Nieck E. Benes**

An interfacial polymerization process is introduced for the fabrication of thermally stable cyclomatrix poly(phenoxy)phosphazenes thin-film composite membranes that can sieve hydrogen from hot gas mixtures. By replacing the conventionally used aqueous phase with dimethyl sulfoxide/potassium hydroxide, a variety of biphenol molecules are deprotonated to aryloxide anions that react with hexachlorocyclotriphosphazene dissolved in cyclohexane to form a thin film of a highly cross-linked polymer film. The film membranes have persistent permselectivities for hydrogen over nitrogen (16–27) and methane (14–30) while maintaining hydrogen permeances in the order of (10^{-8}–10^{-7} mol $m^{-2}s^{-1}Pa^{-1}$) at temperatures as high as 260 °C and do not lose their performance after exposure to 450 °C. The unprecedented thermal stability of these polymer membranes opens the potential for industrial membrane gas separations at elevated temperatures.

1. Introduction

Molecular separations are pervasive in the large-scale chemical industry and energy production sector and denote gigantic energy requirements. More efficient separation methods can have a large impact on the process economics, and more importantly, on their sustainability. For processes that occur at high temperatures, the efficiency can be substantially improved when the necessity to cool and reheat process streams is avoided. Membrane-based separations for hot gases have the potential for this, but producing membranes that have a persisting separation performance at high temperatures is challenging.[1–3] Membrane materials that have been investigated for hot gas separation include inorganic materials (metals, zeolites, carbons),[4–6] 2D layered materials,[7,8] covalent organic frameworks (COFs),[9] and metal–organic frameworks (MOFs).[1,2,10–13] However, their complex and costly production have hampered their industrial application.[7,14,15] Polymeric membranes would offer a more economical and scalable alternative. A limited range of polymeric materials has been investigated, including polybenzimidazole (PBI), polyimide (PI), and thermally rearranged polymers (TRP).[16–22] Shortcomings of these membranes are insufficient permeance and selectivity at high temperatures,[16,17,23] and the need for costly chemical or thermal treatment for network conversion.[23–25] Hybrid membranes, consisting of a network of inorganic polyhedral oligomeric silsesquioxane (POSS) connected via organic imide bridges, have demonstrated good separation performance at elevated temperatures.[26] Similar to the large-scale production of reverse osmosis membranes, these hybrid membranes are fabricated via the facile interfacial polymerization (IP) method, in which a thin layer is formed in situ at the interface of two immiscible phases.[27,28] Unfortunately, these membranes require a thermal imidization step.

Recently, we developed membranes in which POSS cages are connected in a network via hexachlorocyclotriphosphazene (HCCP) bridges.[28] The cyclic phosphazene group offers exceptional inherent properties such as natural flame retardancy and thermal stability.[29–31] Much of the current literature on cyclomatrix polyphosphazene (CPPz) reports supermacromolecular self-assemblies like nano or microspheres, nanosheets, and microtubes.[29,32–36] Limited studies report the successful formation of thin defect-free and continuous CPPz

F. Radmanesh, E. J. R. Sudhölter, M. G. Elshof, N. E. Benes
Membrane Science and Technology Cluster, Faculty of Science and Technology
MESA+ Institute for Nanotechnology
University of Twente
P.O. Box 217, Enschede 7500 AE, The Netherlands
E-mail: n.e.benes@utwente.nl
E. J. R. Sudhölter
Organic Materials & Interfaces, Department of Chemical Engineering
Faculty of Applied Sciences
Delft University of Technology
Delft 2629 HZ, The Netherlands
A. Tena
The European Membrane Institute Twente, Faculty of Science and Technology
University of Twente
P.O. Box 217, Enschede 7500 AE, The Netherlands
A. Tena
Surfaces and Porous Materials (SMAP)
Associated Research Unit to CSIC
Institute of Sustainable Processes (ISP)
Dr. Mergelina S/n
University of Valladolid
Valladolid 47071, Spain

The ORCID identification number(s) for the author(s) of this article can be found under https://doi.org/10.1002/admi.202202077.

DOI: 10.1002/admi.202202077

membrane films.[27,37] The IP process allows not only the formation of such films but also a high degree of crosslinking that moderates the macromolecular dynamics at the elevated temperatures of application. As such, these membranes have much potential for sieving small molecules, such as H_2, from hot gas streams,[26,28] where the C(sp^3) bonds in the propyl groups of the POSS molecules limit the applicable temperature range to 300 °C.

Here, we demonstrate a new strikingly versatile synthesis route for highly cross-linked CPPz-based thin-film composite (TFC) membranes. By replacing the aqueous phase, which is typically used in conventional interfacial polymerizations, with dimethyl sulfoxide (DMSO)/potassium hydroxide (KOH), a range of different, previously nonapplicable, nucleophile monomers can be used for substitution reactions with the HCCP. We focus on a selection of aromatic biphenols. Maaskant et al. reported the polymerization of aromatic biphenols in water with HCCP in dichloromethane. These highly cross-linked CPPz polymers with O-linking atoms exhibit higher thermal stability than materials with N-linking atoms.[27,32] However, the reactivity of the phenols in water is too limited to allow the formation of thin defect-free membrane films. Mayr et al. reported enhanced reactivity of phenols in DMSO as compared to water.[38] The addition of KOH makes the DMSO solution a superbase in which the phenols can easily be deprotonated to become highly soluble and nucleophile phenolates that can react with HCCP.

To demonstrate the broad applicability of this concept, various CPPz membranes are developed from a selection of organic bridges with different ranges of flexibility. The membranes are characterized in terms of the permeance of H_2 and the slightly larger CO_2, CH_2, and N_2, at elevated temperatures. The results aid the molecular design of high-performance CPPz membranes, promoting advances in gas separation applications at elevated temperatures.

2. Results and Discussion

Thin film CPPz were formed using phosphonitrilic chloride trimer (HCCP) in cyclohexane and different aromatic biphenols in the solution of DMSO with KOH (**Figure 1**A,B). The

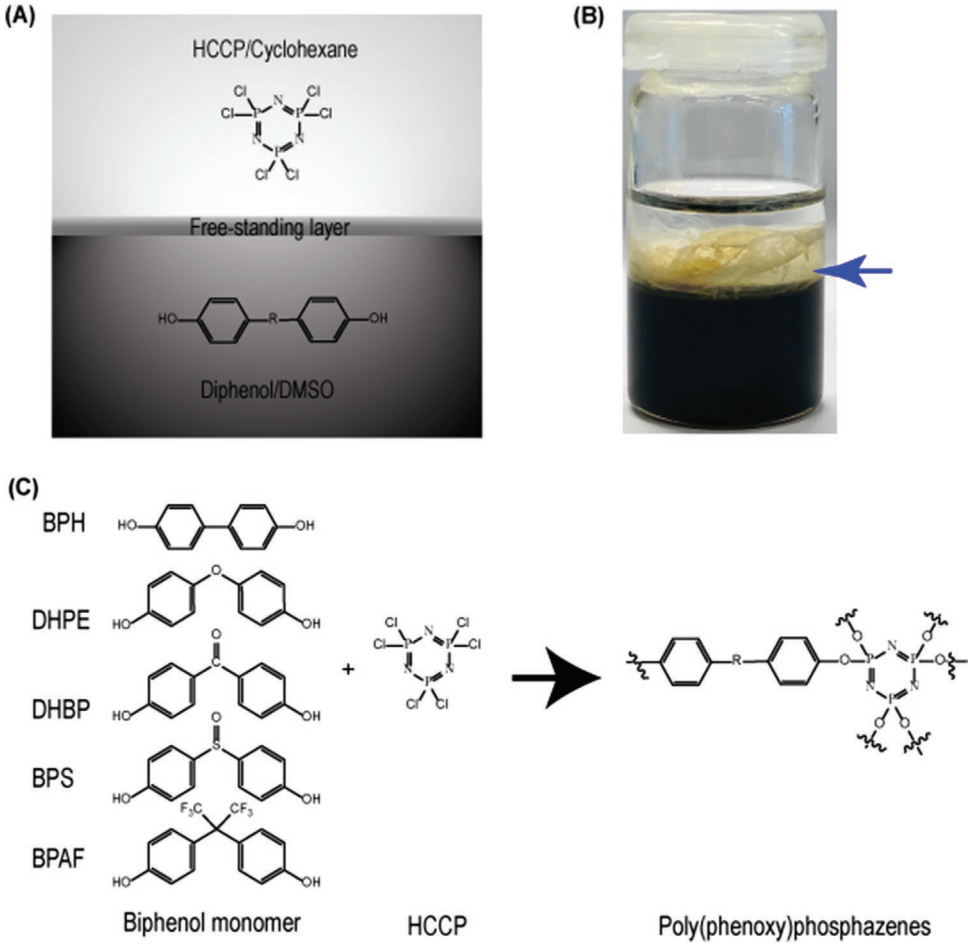

Figure 1. A) Visualization of the interfacial polymerization between HCCP in cyclohexane and the potassium phenoxide of hydroxyl monomers in DMSO. An aromatic biphenol is dissolved in DMSO/KOH solution to convert biphenol into potassium phenoxide. Subsequently, it reacts with HCCP, which is dissolved in cyclohexane. The layer forms at the interface between the two solvents. B) Picture of the interfacial polymerization of a poly(phenoxy)phosphazene at the interface of two monomer phases. C) Synthesis of poly(phenoxy)phosphazenes films through interfacial polymerization between five different hydroxyl compounds and HCCP.

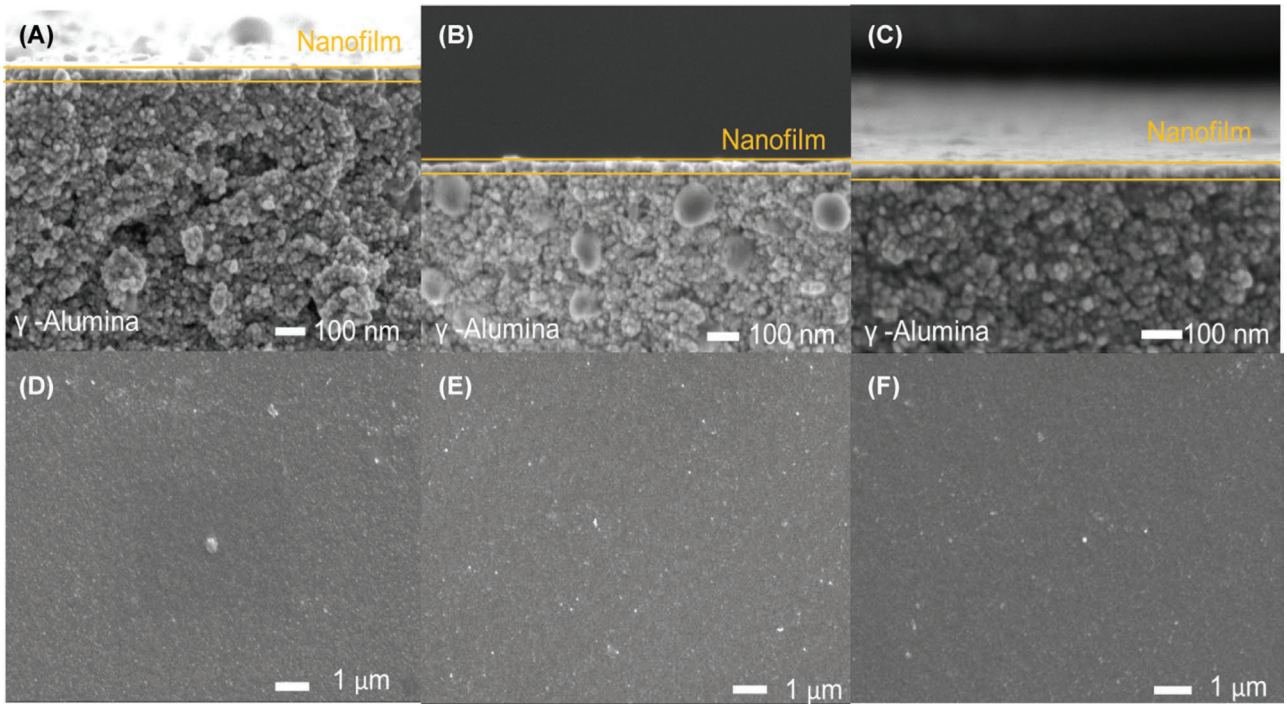

Figure 2. A–C) Cross-sectional FE-SEM images of poly(phenoxy)phosphazenes membranes on alumina support for BPH-HCCP, BPS-HCCP, and BPAF-HCCP, respectively. D–F) Surface FE-SEM images of poly(phenoxy)phosphazenes membranes on alumina supports: BPH-HCCP, BPS-HCCP, and BPAF-HCCP, respectively.

selected biphenols are 4′-dihydroxybiphenyl (BPH), 4,4′-dihydroxydiphenyl ether (DHPE), 4,4′-dihydroxybenzophenone (DHBP), 4,4′-sulfonyldiphenol (BPS), and 4,4′-(Hexafluoroisopropylidene)diphenol (BPAF) (Figure 1C and Figure S1, Supporting Information). The presence of KOH is necessary for the conversion of the biphenols into aryloxide anions. These anions are highly nucleophile, which aids the formation of a thin layer between the two immiscible solvents. The reaction involves the attack of the phenoxides on the P atoms of HCCP, resulting in the formation of CPPz, and KCl as a by-product.

In addition to freestanding films, the CPPz films can also be formed directly atop a porous alumina support structure to assure sufficient mechanical strength for application as a membrane. For this, the porous support is impregnated with the DMSO solution and is then contacted with the HCCP in cyclohexane. **Figure 2**A–C depicts field emission scanning electron microscope (FE-SEM) images of resulting cross sections for three different biphenols and reveals that the thickness of the CPPz layer is ≈30 nm. The top-view images in Figure 2D–F show that the membrane surfaces are smooth and dense, and without evident pinholes or other defects. AFM characterization (Figure S2 and Table S1, Supporting Information) reveals that the surfaces of these three samples have comparable roughness (2.5–4 nm), that is, due to the low thickness of selective layers, similar to that of the unmodified ceramic support (4 nm).

The formation of the poly(phenoxy)phosphazene networks is confirmed by Fourier transform infrared spectroscopy in attenuated total reflectance mode (FTIR-ATR). **Figure 3**A shows the characteristic peaks of P—O—Ar (950 cm^{-1}), the aromatic group (1400 and 1600 cm^{-1}), and two bands of HCCP (a broad peak at 1100 to 1200 and 875 cm^{-1}). Except for the DHPE-HCCP, the FTIR spectra show all typical bands of the biphenol monomers. In the DHBP-HCCP spectrum, the peak at 1650 cm^{-1} is attributed to the carbonyl group of DHBP. In the BPS-HCCP spectrum, the S=O group of BPS appears at 1290 cm^{-1}, and in the BPAF-HCCP spectrum, the CF_3 band appears at 1254 cm^{-1}.[27]

The thermal stability of networks is evaluated by thermo gravimetric analysis in combination with mass spectrometry, TGA-MS (Figure 3B and Figure S3, Supporting Information). A limited mass loss (between 3% and 5%) is detected below 400 °C. This is attributed to the desorption of physically bound solvents (DMSO and water) and the removal of trapped monomers. Continuous mass loss is observed above 400 °C because of organic decomposition, evidenced by the presence of C_3H_3 and C_4H_2 in the mass spectrometer data. The thermal stability of the CPPz is higher as compared to the POSS-HCCP materials presented in our previous study. This is due to the absence of the C(sp^3) of the POSS-propyl group, and the Ar—O—P rather than the C—NH—P connection.[28] At 450 °C, minor traces of HCl evolve, indicating a small amount of unreacted Cl in the networks. Noteworthy to mention is that the amount of HCl is far lower than in the previous study by Maaskant et al.,[27] evincing the great extent of crosslinking in our networks. BPH-HCCP shows a limited continuous release of aromatic fragments and CO_2, and a slight reduction in the ratio of C/P (energy dispersive X-ray spectra [EDX], Tables S2 and S3, Supporting Information) at 800 °C. Conversely, for BPAF-HCCP, all fluorine is removed during TGA, and only C and P elements remain after the thermal procedure. The order for the residues mass of the networks at 800 °C is BPH-HCCP>DHBP-HCCP> DHPE-HCCP> BPS-HCCP> BPAF-HCCP.

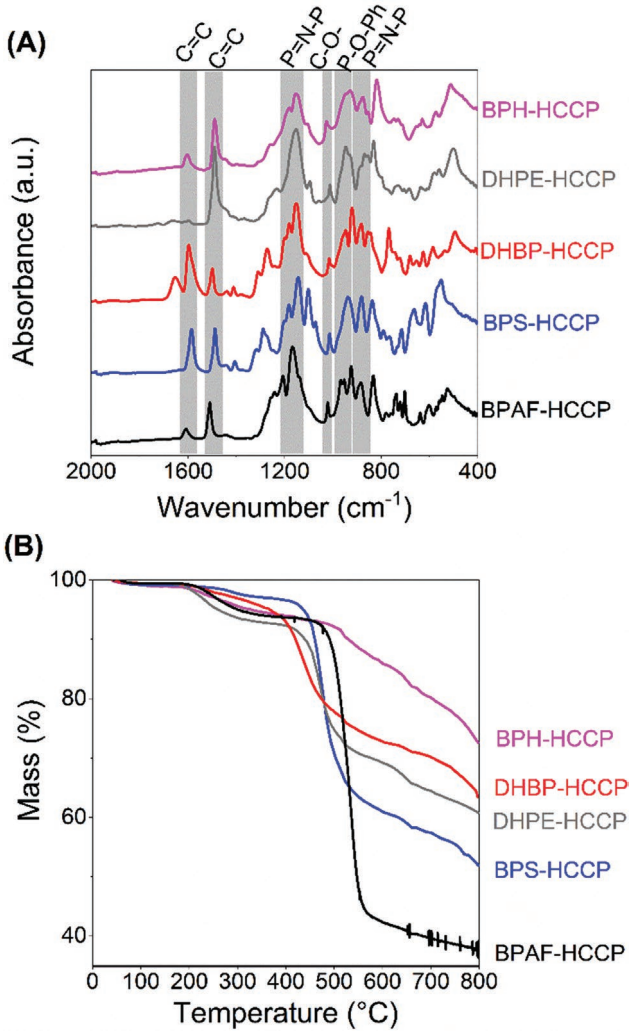

Figure 3. A) FTIR spectra and B) TGA of the formed poly(phenoxy)phosphazenes network synthesized via interfacial polymerization under an N_2 atmosphere obtained with a heating rate of 10 °C min^{-1}.

For HCCP, it is well-known that the rings can be opened at a temperature exceeding 250 °C.[39] For the cross-linked materials, FTIR data does not reveal whether cyclic phosphazene rings remain after exposure to high temperatures. To unravel this, two small molecules, hexaphenoxycyclotriphosphazene (ArO_6PP) and triphenoxy trichlorocycoltriphosphazene (ArO_3Cl_3PP), that are representative of the molecular structure of the CPPz have been characterized by FTIR and ^{31}P nuclear magnetic resonance (NMR), before and after heat treatment at 260 °C for 10 h under N_2. The FTIR spectra obtained before and after thermal treatment (Figure S4, Supporting Information) are very similar, with peaks corresponding to P=N−P asymmetric (1100 to 1200 cm^{-1}) and symmetric stretching (875 cm^{-1}),[29] and the P−O−Ar bond (950 cm^{-1}).[40] For ArO_3Cl_3PP, the intensity of the P−O−Ar peak increases during temperature exposure due to the substitution of Cl by ArOH residues that are present in the samples. The NMR spectra for ArO_6PP (Figure S5, Supporting Information) before and after heat treatment are interchangeable. For ArO_3Cl_3PP (Figure S6, Supporting Information), the peaks at $\delta = 0$–5 disappear, and the peaks from $\delta = 14.1$–18.1 ppm shift to $\delta = 18.1$–20.5, indicating the substitution of Cl by ArO.[41,42] The results imply that phosphazene rings with ArO rather than Cl groups remain cyclic at 260 °C.

In addition to high thermal stability, a molecular sieving ability of a polymer film at elevated temperatures requires that the macromolecular dynamics of the material under such conditions are moderated. For this, a sufficient degree of crosslinking is vital. X-ray fluorescence (XRF) spectroscopy was used to screen the extent of crosslinking from the relative presence of the elements P, Cl, S, and K (**Table 1**), combined with C,N analysis for the elements C and N (**Table 2**). The XRF data reveal the presence of S and K that can be attributed to residual DMSO and KOH. The high ratios of P/Cl (2.4–23.3) indicate that almost all Cl has reacted with the biphenolates. This is confirmed by the ratio of C/N, which varies between 2 and 3.5. By considering the number of C present in the biphenols, this infers that highly cross-linked networks are formed with, for BPH, DHPE, BPS, and DHBP, on average, at least five connecting organic bridges between the phosphazene rings. For BPAF, the degree of crosslinking is slightly less, and a relatively high Cl concentration is observed.

The permeance of small gas molecules through the thin film membranes reveals persisting molecular sieving ability; for all membranes, a decrease of permeance with increasing kinetic diameter of the molecule is observed at temperatures from 50 to 260 °C (**Figure 4**A and Figure S7, Supporting Information). This behavior is similar to that of glassy polymers and originates from large differences in the diffusion rates for molecules of slightly different sizes and shapes.[45,46] In essence, for slightly larger molecules, the jump rate between bordering open spaces in a rigid glassy polymer decreases strongly. For

Table 1. XRF Elemental concentration (%) for poly(phenoxy)phosphazenes free-standing films.

Element[a)]	BPH-HCCP	DHPE-HCCP	DHBP-HCCP	BPS-HCCP	BPAF-HCCP
P	56.4 ± 0.8	45.1 ± 0.9	45.7 ± 0.9	27.8 ± 0.9	50.9 ± 1
Cl	5 ± 3.6	18.6 ± 2.1	6.4 ± 3.7	1.2 ± 10.7	15.8 ± 2.5
S	0.4 ± 0	20.3 ± 2.1	26.1 ± 1.2	56.9 ± 0.7	1.6 ± 6.6
K	36.7 ± 1	14.2 ± 2.1	20.2 ± 1.6	2.7 ± 4.6	29.3 ± 1.6
P/Cl	11.3	2.4	7.1	23.3	3.2
Unreacted Cl per HCCP	0.3	1.2	0.4	0.1	1

[a)]Reported errors for XRF data are the relative statistical errors of the peaks.

Table 2. C,N elemental analysis (%) for poly(phenoxy)phosphazenes free-standing films.

Element[a)]	BPH-HCCP	DHPE-HCCP	DHBP-HCCP	BPS-HCCP	BPAF-HCCP
C	40.1 ± 0.5	51.6 ± 0.5	53.7 ± 0.3	47.4 ± 0.3	36.3 ± 0.3
N	2.8 ± 0	4.7 ± 0.1	4.1 ± 0	3.8 ± 0	3.8 ± 0
C/N	14.3 ± 0.2	11 ± 0.3	13.1 ± 0.1	12.5 ± 0.1	9.6 ± 0.1
Organic bridge per HCCP	3.5 ± 0.1	2.7 ± 0.1	3 ± 0	3 ± 0.1	2 ± 0

[a)]Reported errors for XRF data are the relative statistical errors of the peak.

polyphosphazene polymers, it has been demonstrated that the T_g can be affected by introducing different substitution groups.[47–50] In our case, the high degree of crosslinking aids in moderating the dynamics of the macromolecular network, enabling molecular sieving at high temperatures.

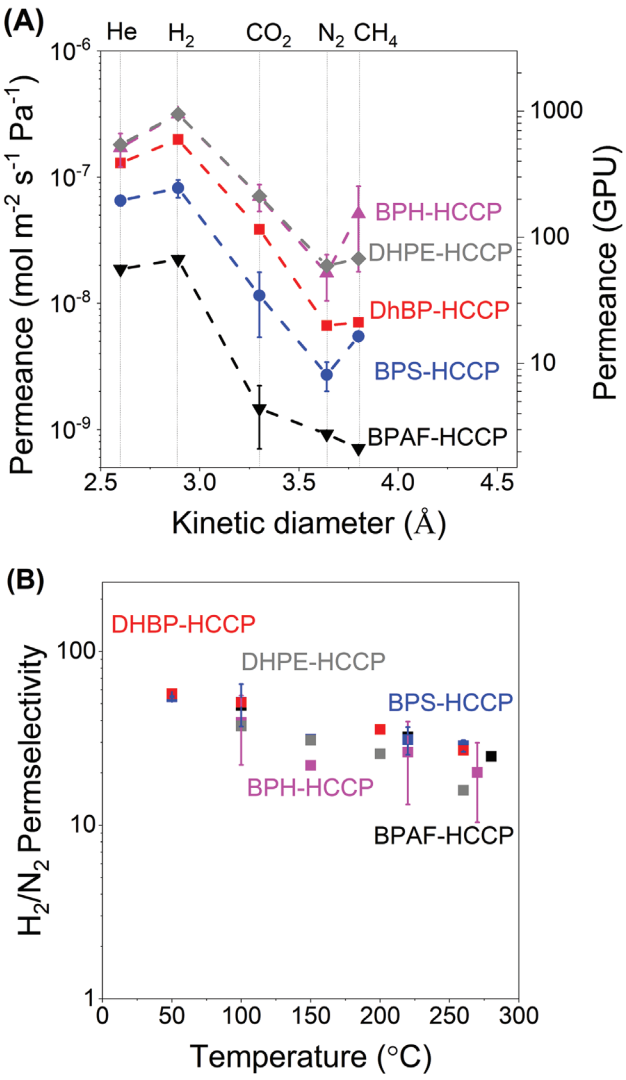

Figure 4. A) Gas permeance as a function of gas kinetic diameter derived from BPH-HCCP, DhPE-HCCP, DHBP-HCCP, BPS-HCCP, and BAF-HCCP. All the measurements were done at a transmembrane pressure of 2 bar and a temperature of 260 °C. B) The ideal H_2/N_2 permselectivity of the membranes as a function of temperature.

The H_2 permeances are in the range of 2.3×10^{-8} to 3.2×10^{-7} mol m^{-2} s^{-1} Pa^{-1} (69 to 943 GPU) at 260 °C. For all gasses, the permeance follows the order BPH-HCCP, DHPE-HCCP > DHBP-HCCP > BPS-HCCP > BAF-HCCP. Strikingly, the permselectivities are quite similar for all membranes. In Figure 4B, the permselectivity of H_2/N_2 is plotted versus temperature. The permselectivity of H_2/CH_4 is of a similar order as that of H_2/N_2 (Figure S8, Supporting Information). The permselectivities decrease with temperature because the activation energies of the diffusion coefficients of larger molecules in rigid polymer matrices are generally larger. In the BPH, BHDP, and BPS-based membranes, the activation energies of the small H_2 and He are in the range of 14.2–17.9 kJ mol^{-1}, while those of the bigger N_2 and CH_4 are in the range of 21.3–23.7 kJ mol^{-1} (Figure S9 and Table S4, Supporting Information). These values are comparable to those of polyimide and poly(p-phenylene benzobisimidazole) membranes.[17,28,52,53] For the BPAF-based membrane, the values are somewhat lower. It should be noted that even at 260 °C, the H_2/N_2 and H_2/CH_4 permselectivities of all membranes still exceed the value of 10, which is remarkable for polymer-based membranes. The permselectivities of H_2/CO_2 are in the range of 2–10, which is lower as compared to the other gas pairs, and do not show a decrease with temperature. For CO_2, the energy of activation is relatively low because of the more pronounced dispersion interactions of this molecule with the polymer materials; the heat of sorption of the CO_2 will be larger and the slope of Arrhenius type temperature dependence of sorption has the opposite sign as compared to diffusion.

The similar activation energies and permselectivities of the membranes imply that differences in their permeance values result from differences in the morphology and thicknesses of the membranes, affecting the distances that the molecules must travel, rather than from distinct molecular structures of the materials, affecting the diffusion rate. SEM images reveal no substantial differences in the thicknesses of the films atop the porous support structure that can explain the permeance differences. Likely, polymerization also occurs inside the small pores of the support, strongly reducing the permeance values. In classical interfacial processes, polymerization is known to occur predominantly in the nonpolar phase rather than in the aqueous phase. By using DMSO instead of water, the location of the polymerization reaction may shift to the polar phase, resulting in a more pronounced growth in the pores of the support. The extent of film growth is strongly affected by the conditions of the process, impacting the evolution of reaction kinetics and transport kinetics during film formation. By increasing the amount of KOH, such effects can become evident.[54] When the KOH concentration is increased around twofold, the permeances of the gases decrease several orders of magnitude (Table S5, Supporting Information). Compared to the lower KOH concentration, FE-SEM does not show any variations in the thickness atop ceramic supports, and XRF and CN analysis reveal a similar extent of crosslinking for freestanding films (Tables S6 and S7, Supporting Information). This agrees with the possibility of more pronounced growth into the porous structure. It is also observed that by lowering the KOH concentration, higher permeances can be achieved, but obtaining

Table 3. Summary of the performance of different membranes.

Membrane material	Thickness [nm]	T [°C]	Analysis	H_2 permeance [GPU]	H_2/CO_2	H_2/N_2	H_2/CH_4	Ref.
Poly(phenoxy) phosphazene-BPH based	20–30	260	Pure	950	4	20	15	This work
Poly(phenoxy) phosphazene-BPS based	20–30	260	Pure	300	8	30	20	This work
POSS-HCCP	78	250	Pure	1000	7.1	40	31	[28]
PolyPOSS-imide(6FDA)	100	250	Pure	600	5	10	10	[26]
TRP	30 000–40 000	210	Pure	0.03	6.2	–	–	[18]
PolyPOSS-imide(PMDA)	100	200	Pure	180	10	100	80	[44]
PBI-Pd NPs	800	200	Mixture	1.25	40	–	–	[43]
2D COF	2000	200	Mixture	≈5500	16	–	–	[9]
MOFs (ZIF-8)	20 000	150	Pure	648	10.3	17.6	34.8	[13]
Covalent organic nanosheet (CON)	41	150	Pure	2566	26.2	40.5	74.2	[7]
Cross-linked PI	15 000	150	Pure	≈7	10	–	–	[51]
PBDI (poly(p-phenylene) benzobisimidazole)	1300	100	pure	71.7	18.9	59.7	47.5	[17]
PI	30 000–50 000	100	Pure	1.8×10^{-10}	≈5.2	80	–	[52]

a defect-free thin film for these lower concentrations is more challenging.

The persisting permselectivities at 260 °C are exceptional. In **Table 3**, the performance of different membranes at elevated temperatures is summarized. As compared to the CPPz membranes, the very elegant iCON-based membranes[7] have higher permeance values up to 150 °C, but no data are available for their performance at higher temperatures. For temperatures exceeding 200 °C, the polyPOSSimide membranes[26,44] show comparable selectivity and lower permselectivities, while the polyPOSS-HCCP membranes[28] show similar permeance with about twofold higher permselectivity.

In contrast to the POSS-based membranes, the CCPz membranes are prepared from more inexpensive and more readily available monomers in a single-step reaction. Also, the membranes lack the C(sp^3) bond of the POSS-propyl group and have Ar—O—P rather than C—NH—P connections, providing inherently higher thermal stability. For the POSS-based membranes, the maximum application temperature is 300 °C.[28] Figures S10 and S11, Supporting Information, show that the permeance and permselectivity of the CCPz membranes are unaffected after the membranes have been exposed to 350 and 450 °C for 10 h.

3. Conclusion

In conclusion, we have developed ultrathin (≈20–30 nm) cyclomatrix poly(phenoxy)phosphazene membranes for the first time via interfacial polymerization using several biphenols including BPH, DHPE, DHBP (Sigma-Aldrich), 4,4′-sulfonyldiphenol (BPS), 4,4′-(Hexafluoroisopropylidene)diphenol (BPAF), and HCCP. The membranes are highly cross-linked and thermally stable up to 450 °C. They show persisting molecular sieving behavior up to 260 °C, which is the temperature limit of our sealings, with permselectivities of H_2 over N_2 and CH_4. The performance of the membranes remains unchanged after exposing them to 350 and 450 °C for 10 h. There are currently very limited alternative polymer-based membranes that have comparable performance at this high temperature, and these require more complex and expensive fabrication. Our facile fabrication process allows for using monomers that cannot be used in conventional interfacial polymerizations, granting access to a broader assortment of membrane materials with the potential for industrial separations under harsh conditions.

4. Experimental Section

Materials: Phosphonitrilic chloride trimer (HCCP, 99%, Sigma-Aldrich), hexaphenoxycyclotriphosphazene (ArO_6PP, >98%, TCI), BPH (Sigma-Aldrich), DHPE (Sigma-Aldrich), DHBP (Sigma-Aldrich), 4,4′-sulfonyldiphenol (BPS, Sigma-Aldrich), 4,4′-(Hexafluoroisopropylidene)diphenol (BPAF, Sigma-Aldrich), phenol (Sigma-Aldrich), tetrahydrofuran (anhydrous, ≥99.9%, Sigma-Aldrich), DMSO (anhydrous, ≥99.9%, Sigma-Aldrich), cyclohexane (EMSURE for analysis, Merck), sodium hydroxide (NaOH, reagent grade, Sigma-Aldrich), and potassium hydroxide (KOH, pellets extra pure, Merck) were used as received. Porous α-alumina discs (Ø 39 mm, thickness 2 mm) were obtained from Pervatech B.V. and used as support.

CCPz Fabrication: Freestanding polymer layers and TFC polymeric membranes were formed by interfacial polymerization of 1) a 10 w/v% solution of the corresponding biphenols in DMSO containing KOH (super base);[55] molar ratio of biphenol:KOH of 0.5, that is, stoichiometric with respect to phenol groups, and 0.75, that is, substoichiometric with respect to phenol groups and 2) a 3.5 w/v% HCCP solution in cyclohexane.

Unless otherwise mentioned, a molar ratio of biphenol:KOH of 0.75 was used. That means that a maximal two of every three phenol groups can be deprotonated to phenolate anions. The used concentrations of biphenols and HCCP and the applied volumes reflected (if the solutions were perfectly mixed) a molar stoichiometry of HCCP:biphenol ≈1:5 since HCCP contained six reactive chlorine atoms and the biphenols had two phenol groups. The molar ratio of reactive chlorine to phenol was 6:10. Since the molar ratio of biphenol:KOH was 0.75, the molar ratio of reactive chlorine to phenolate anion was ≈1:1. If all the reactive chlorine would be displaced by phenolate anion substitution, there were still unreacted phenol groups present (≈1/3 of the number of biphenol moieties). Since the performed polymerization happened at the interface, such an ideal situation does not exist, and some heterogeneity will be present in the formed membrane layers.

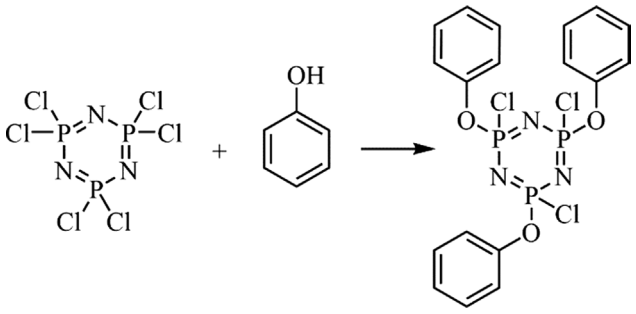

Figure 5. Formation of a triphenoxy trichlorocyclotriphosphazene by the reaction of phenol with HCCP.

Synthesis of CCPz Freestanding Films: After heating biphenol solutions at 80 °C for 2 h, 10 mL was mixed with the HCCP solution (10 mL) and vigorously stirred for 10 min. The formed suspension was filtered, washed with water, ethanol, and acetone, and dried in the vacuum oven at 50 °C.

Preparation of Biphenol-HCCP Thin-Film Composite Membranes: The CCPz membranes were prepared atop ceramic supports: α-alumina discs with a 3-µm-thick γ-alumina layer (pore size of 3–5 nm) with the setup described elsewhere.[28] First, the biphenol solution and support were heated at 80 °C for 2 h and 30 min, respectively. After this, the preheated ceramic was soaked in preheated biphenol solution for 15 min at 80 °C. Subsequently, the support surface was dried by applying a rubber roller and N_2 gun, followed by contacting it with the HCCP solution for 10 min at ambient temperature. After removing the HCCP solution, the membranes were rinsed with ethanol. Before further analysis, the membrane was kept under a fume hood overnight and then dried in a vacuum oven at 50 °C for a minimum of 24 h.

Synthesis of Triphenoxy Trichlorocycoltriphosphazene (ArO_3Cl_3PP): Triphenoxy trichlorocycoltriphosphazene was prepared according to the literature, with some modifications, **Figure 5**.[41,56] HCCP was reacted with an excess amount of sodium phenolate. For this purpose, a suspension of NaOH (0.85 g, 0.02 mol), phenol (2 g, 0.02 mol), HCCP (2.5 g, 0.007 mol), and 40 mL of THF was prepared in a 100-mL three-necked round-bottom flask. The mixture was refluxed for 5 h under a nitrogen atmosphere. After the reaction was completed, the suspension was distilled under reduced pressure with a rotary evaporator, and the remaining crude product was washed with hot deionized water to give a light yellow solid product. The product was dried at 50 °C under a vacuum overnight. ^{1}H NMR (400 MHz, chloroform) δ (11.7–12.17), ^{31}P NMR (162 MHz, Chloroform-d) δ 16.13, 15.76 (d, J = 14.8 Hz), 15.57–15.31 (m), 15.15, 3.82, 3.53 (d, J = 14.3 Hz), 3.28, 2.65, 2.40–1.95 (m), 1.90, 1.64 (d, J = 18.5 Hz), 1.27, 1.18–0.07 (m). The product was mostly a mixture of diphenoxy, symmetrical triphenoxy, and asymmetrical triphenoxy.[41] Besides, a small trace of phenol can be observed, ^{1}H NMR (400 MHz, chloroform) (7.22 (s, 2H), 6.55–6.44 (m, 3H)).

Material Characterization: An FE-SEM (Zeiss MERLIN) was used to evaluate the thickness and morphology of the supported membranes. For cross-section images, samples were immersed in liquid nitrogen for 5 min and carefully broken to reveal the full cross-section. All samples were mounted on an FE-SEM holder using double-sided carbon tape and coated with a 5 nm Pt/Pd conductive layer using a sputter coater Quorum Q150T ES (Quorum Technologies, Ltd., UK). EDX was taken with a JEOL-JSM6010 SEM. For this purpose, the obtained free-standing films were coated with a 5 nm Pt/Pd conductive layer prior to imaging using a sputter coater Quorum Q150T ES (Quorum Technologies, Ltd., UK). EDX analysis was performed at 10 kV with >1000 counts s^{-1}. The experiment was repeated three times at different points, and the average value was reported. 1H, 13C, and 31P NMR spectroscopies were performed on a 400 MHz pulsed Fourier transform NMR spectrometer (Agilent 400-MR DD2) using deuterated DMSO (DMSO-d6). FTIR-ATR (PerkinElmer Spectrum Two, USA) was used to characterize the free-standing films. Spectra were averaged over 16 scans with a resolution of 4 cm^{-1} over a wavelength range from 400 to 4000 cm^{-1}. The elemental composition of synthesized free-standing films was measured with XRF (S8 Tiger, Bruker) and CN elemental analysis (FLASH 2000 series analyzer). The thermal stability of the membranes was examined by heating a fixed amount of sample (10 mg) on a heating stage under an inert nitrogen atmosphere at a heating rate of 10 °C min^{-1} using a TGA (STA 449 F3 Jupiler, Netzsch) in combination with MS (QMS 403 D Aeolos MS, Netzsch) to detect the released gaseous products according to their mass to charge ratios (m/z = 1–110 amu).

Membrane Performance: Single gas permeance measurements were performed using a gas permeation setup in dead-end mode (Convergence Inspector Poseidon). The single gas permeance of He (0.255 nm), H_2 (0.289 nm), CO_2 (0.33 nm), N_2 (0.364 nm), and CH_4 (0.389 nm) was measured at a transmembrane pressure of 2 bar within the temperature range from 50 to 260 °C, which is limited by the thermal stability of the sealing. The permselectivity was calculated as the ratio of the respective permeances. The experiments were performed at least twice, and the reported results are the average of the obtained values.

Supporting Information

Supporting Information is available from the Wiley Online Library or from the author.

Acknowledgements

This work is part of the GENESIS project and the authors acknowledge the financial support from the European Union's Horizon 2020 Research and Innovation Program under Grant Agreement No. 760899.

Conflict of Interest

The authors declare no conflict of interest.

Data Availability Statement

The data that support the findings of this study are openly available in 4TU research at https://doi.org/10.4121/21082006, reference number 21082006.

Keywords

gas separation, high temperature, interfacial polymerization, membranes, polyphosphazenes

Received: September 20, 2022
Revised: October 14, 2022
Published online:

[1] Y. Wang, H. Jin, Q. Ma, K. Mo, H. Mao, A. Feldhoff, X. Cao, Y. Li, F. Pan, Z. Jiang, *Angew. Chem., Int. Ed.* **2020**, *59*, 4365.
[2] H. Fan, M. Peng, I. Strauss, A. Mundstock, H. Meng, J. Caro, *Nat. Commun.* **2021**, *12*, 38.
[3] M. G. Schultz, *Science* **2003**, *302*, 624.
[4] P. Kumar, D. W. Kim, N. Rangnekar, H. Xu, E. O. Fetisov, S. Ghosh, H. Zhang, Q. Xiao, M. Shete, J. I. Siepmann, T. Dumitrica, B. McCool, M. Tsapatsis, K. A. Mkhoyan, *Nat. Mater.* **2020**, *19*, 443.

[5] C. Kura, Y. Kunisada, E. Tsuji, C. Zhu, H. Habazaki, S. Nagata, M. P. Müller, R. A. De Souza, Y. Aoki, *Nat. Energy* **2017**, *2*, 786.
[6] W. H. Chen, Z. Y. Chen, S. Lim, Y. K. Park, P. L. Show, *Int. J. Hydrogen Energy* **2021**, https://doi.org/10.1016/j.ijhydene.2021.07.182.
[7] Y. Ying, M. Tong, S. Ning, S. K. Ravi, S. B. Peh, S. C. Tan, S. J. Pennycook, D. Zhao, *J. Am. Chem. Soc.* **2020**, *142*, 4472.
[8] L. Ding, Y. Wei, L. Li, T. Zhang, H. Wang, J. Xue, L.-X. Ding, S. Wang, J. Caro, Y. Gogotsi, *Nat. Commun.* **2018**, *9*, 155.
[9] H. Fan, M. Peng, I. Strauss, A. Mundstock, H. Meng, J. Caro, *J. Am. Chem. Soc.* **2020**, *142*, 6872.
[10] Y.-S. Li, H. Bux, A. Feldhoff, G.-L. Li, W.-S. Yang, J. Caro, *Adv. Mater.* **2010**, *22*, 3322.
[11] Y. S. Li, F. Y. Liang, H. Bux, A. Feldhoff, W. S. Yang, J. Caro, *Angew. Chem.* **2010**, *122*, 558.
[12] A. Huang, J. Caro, *Angew. Chem., Int. Ed.* **2011**, *50*, 4979.
[13] Q. Liu, N. Wang, J. Caro, A. Huang, *J. Am. Chem. Soc.* **2013**, *135*, 17679.
[14] M. A. Habib, A. Harale, S. Paglieri, F. S. Alrashed, A. Al-Sayoud, M. V. Rao, M. A. Nemitallah, S. Hossain, M. Hussien, A. Ali, M. A. Haque, A. Abuelyamen, M. R. Shakeel, E. M. A. Mokheimer, R. Ben-Mansour, *Energy Fuels* **2021**, *35*, 5558.
[15] S. Yuan, X. Li, J. Zhu, G. Zhang, P. Van Puyvelde, B. Van der Bruggen, *Chem. Soc. Rev.* **2019**, *48*, 2665.
[16] Y. Jin, B. Gao, C. Bian, X. Meng, B. Meng, S. I. Wong, N. Yang, J. Sunarso, X. Tan, S. Liu, *Green Chem.* **2021**, *23*, 3374.
[17] M. Shan, X. Liu, X. Wang, Z. Liu, H. Iziyi, S. Ganapathy, J. Gascon, F. Kapteijn, *J. Mater. Chem.* **2019**, *7*, 8929.
[18] S. H. Han, H. J. Kwon, K. Y. Kim, J. G. Seong, C. H. Park, S. Kim, C. M. Doherty, A. W. Thornton, A. J. Hill, Á. E. Lozano, K. A. Berchtold, Y. M. Lee, *Phys. Chem. Chem. Phys.* **2012**, *14*, 4365.
[19] Y. S. Do, J. G. Seong, S. Kim, J. G. Lee, Y. M. Lee, *J. Memb. Sci.* **2013**, *446*, 294.
[20] L. Zhu, M. T. Swihart, H. Lin, *Energy Environ. Sci.* **2018**, *11*, 94.
[21] Y. Zhuang, J. G. Seong, Y. S. Do, W. H. Lee, M. J. Lee, Z. Cui, A. E. Lozano, M. D. Guiver, Y. M. Lee, *Chem. Commun.* **2016**, *52*, 3817.
[22] K. M. Rodriguez, S. Lin, A. X. Wu, G. Han, J. J. Teesdale, C. M. Doherty, Z. P. Smith, *Angew. Chem., Int. Ed.* **2021**, *60*, 6593.
[23] J. Lee, J. S. Kim, S. Moon, C. Y. Park, J. F. Kim, Y. M. Lee, *J. Memb. Sci.* **2020**, *595*, 117535.
[24] D. Lin, Y. Liu, Z. Jia, S. Qi, D. Wu, *J. Phys. Chem. B* **2020**, *124*, 7969.
[25] S. Kim, J. Hou, Y. Wang, R. Ou, G. P. Simon, J. G. Seong, Y. M. Lee, H. Wang, *J. Mater. Chem.* **2018**, *6*, 7668.
[26] M. J. T. Raaijmakers, M. A. Hempenius, P. M. Schön, G. J. Vancso, A. Nijmeijer, M. Wessling, N. E. Benes, *J. Am. Chem. Soc.* **2014**, *136*, 330.
[27] E. Maaskant, H. Gojzewski, M. A. Hempenius, G. J. Vancso, N. E. Benes, *Polym. Chem.* **2018**, *9*, 3169.
[28] F. Radmanesh, M. G. Elshof, N. E. Benes, *ACS Appl. Mater. Interfaces* **2021**, *13*, 8960.
[29] P. Mohanty, L. D. Kull, K. Landskron, *Nat. Commun.* **2011**, *2*, 401.
[30] A.-M. Caminade, A. Hameau, J.-P. Majoral, *Dalton Trans.* **2016**, *45*, 1810.
[31] M. Zhang, Y. Li, C. Bai, X. Guo, J. Han, S. Hu, H. Jiang, W. Tan, S. Li, L. Ma, *ACS Appl. Mater. Interfaces* **2018**, *10*, 28936.
[32] X. Guo, Y. Li, M. Zhang, K. Cao, Y. Tian, Y. Qi, S. Li, K. Li, X. Yu, L. Ma, *Angew. Chem.* **2020**, *132*, 22886.
[33] X. Wei, D. Zheng, M. Zhao, H. Chen, X. Fan, B. Gao, L. Gu, Y. Guo, J. Qin, J. Wei, Y. Zhao, G. Zhang, *Angew. Chem., Int. Ed.* **2020**, *59*, 14639.
[34] X. Wei, D. Zheng, M. Zhao, H. Chen, X. Fan, B. Gao, L. Gu, Y. Guo, J. Qin, J. Wei, Y. Zhao, G. Zhang, *Angew. Chem.* **2020**, *132*, 14747.
[35] R. Jiang, B. Deng, L. Pi, L. Hu, D. Chen, Y. Dou, X. Mao, D. Wang, *ACS Appl. Mater. Interfaces* **2020**, *12*, 57870.
[36] L. Zhu, X. Huang, X. Tang, *Macromol. Mater. Eng.* **2006**, *291*, 714.
[37] M. You, W. Li, Y. Pan, P. Fei, H. Wang, W. Zhang, L. Zhi, J. Meng, *J. Memb. Sci.* **2019**, *592*, 117371.
[38] R. J. Mayer, M. Breugst, N. Hampel, A. R. Ofial, H. Mayr, *J. Org. Chem.* **2019**, *84*, 8837.
[39] H. R. Allcock, C. Chen, *J. Org. Chem.* **2020**, *85*, 14286.
[40] A. M. Turner, A. Bergantini, M. J. Abplanalp, C. Zhu, S. Góbi, B.-J. Sun, K.-H. Chao, A. H. H. Chang, C. Meinert, R. I. Kaiser, *Nat. Commun.* **2018**, *9*, 3851.
[41] M. Sunitha, C. Reghunadhan Nair, K. Krishnan, K. Ninan, *Thermochim. Acta* **2001**, *374*, 159.
[42] H. R. Allcock, A. A. Dembek, J. L. Bennett, I. Manners, M. Parvez, *Organometallics* **1991**, *10*, 1865.
[43] L. Zhu, D. Yin, Y. Qin, S. Konda, S. Zhang, A. Zhu, S. Liu, T. Xu, M. T. Swihart, H. Lin, *Adv. Funct. Mater.* **2019**, *29*, 1904357.
[44] M. J. T. Raaijmakers, M. Wessling, A. Nijmeijer, N. E. Benes, *Chem. Mater.* **2014**, *26*, 3660.
[45] R. C. Dutta, S. K. Bhatia, *ACS Appl. Polym. Mater.* **2019**, *1*, 1359.
[46] Z. Liu, Y. Liu, W. Qiu, W. J. Koros, *Angew. Chem.* **2020**, *132*, 14987.
[47] X. Zhou, S. Qiu, W. Xing, C. S. R. Gangireddy, Z. Gui, Y. Hu, *ACS Appl. Mater. Interfaces* **2017**, *9*, 29147.
[48] Z. Wang, Y. Zhang, C. Wang, X. Zheng, Y. Zheng, L. Gao, C. Yang, Y. Li, L. Qu, Y. Zhao, *Adv. Mater.* **2020**, *32*, 1907355.
[49] A. K. Sekizkardes, V. A. Kusuma, J. S. McNally, D. W. Gidley, K. Resnik, S. R. Venna, D. Hopkinson, *J. Mater. Chem.* **2018**, *6*, 22472.
[50] H. R. Allcock, *Science* **1976**, *193*, 1214.
[51] M. Omidvar, C. M. Stafford, H. Lin, *J. Membr. Sci.* **2019**, *575*, 118.
[52] O. C. David, D. Gorri, A. Urtiaga, I. Ortiz, *J. Membr. Sci.* **2011**, *378*, 359.
[53] S. Escorihuela, A. Tena, S. Shishatskiy, S. Escolástico, T. Brinkmann, J. Serra, V. Abetz, *Membranes* **2018**, *8*, 16.
[54] H. S. Wu, S. S. Meng, *Chem. Eng. Sci.* **1998**, *53*, 4073.
[55] A. S. Bobkov, N. M. Vitkovskaya, B. A. Trofimov, *J. Org. Chem.* **2020**, *85*, 6463.
[56] N. N. Tian, L. S. Wang, M. Y. Li, Y. Li, R. Y. Jiang, *J. Chem. Eng. Data* **2011**, *56*, 661.